A Comprehensive Pilot Model for Voluntary/Involuntary Action in Rotorcraft-Pilot Coupling

Pierangelo Masarati
Associate Professor
Politecnico di Milano
Milano, Italy

Vincenzo Muscarello
Post Doc
Politecnico di Milano
Milano, Italy

Giuseppe Quaranta
Assistant Professor
Politecnico di Milano
Milano, Italy

Paolo Marguerettaz
PhD Fellow
Politecnico di Torino (now at AgustaWestland)
Torino, Italy

Giorgio Guglieri
Associate Professor
Politecnico di Torino
Torino, Italy

Linghai Lu
Research Assistant
The University of Liverpool,
Liverpool, United Kingdom

Michael Jump
Senior Lecturer
The University of Liverpool,
Liverpool, United Kingdom

ABSTRACT

This work proposes a helicopter pilot model identified from experimental results obtained in piloted simulation flight tests. The tests were originally designed to verify predicted unstable pilot-vehicle systems. The results have been further analyzed using methods for the detection of pilot induced oscillation that are available from the literature. The results show that a pilot-assisted oscillation event occurring in one configuration is characterized by a change of biomechanical properties of the pilot. It is conjectured that such change is triggered by a change in the task of the pilot induced by the specific maneuver that is requested of the pilots in the tests.

INTRODUCTION

The interaction of the pilot with the dynamics of a helicopter is characterized not only by voluntary activity, which is intended to produce the control inputs required to perform a specific task, but also by unintended, involuntary actions. The latter are generally the consequence of vibration being transmitted from the vehicle to the pilot via the cockpit and into the control inceptors. Such vibratory motion is filtered by the pilots' biomechanical characteristics and may produce involuntary control inputs (so-called biodynamic feedthrough, BDFT). These close an undesired control loop, causing adverse rotorcraft pilot couplings (RPC). This aspect of pilot-vehicle interaction is often overlooked during the design phase of the vehicle's life cycle. A recent review of the state of the art in this area can be found in Ref. 1.

An important aspect of a pilot's biomechanics that characterizes BDFT is its dependence upon the task that the pilot is trying to accomplish (Ref. 2). During the European project ARISTOTEL[1] (Refs. 3, 4), several flight simulator tests were performed to investigate RPC in relation to both voluntary and involuntary pilot actions, which can result in so-called Pilot-Induced Oscillations (PIO) and Pilot-Assisted Oscillations (PAO) respectively.

During a test campaign that focused on RPC related to the roll axis (Refs. 5, 6), rigid-body (RB) and aeroelastic (AE) helicopter models representative of the BO105 were flown by professional test pilots in a flight simulator at the University of Liverpool. The aim was to verify the predicted onset of an aeromechanical instability caused by the interaction between the biomechanics of the pilot/control device and the dynamics of the vehicle related to the main rotor blade dynamics (the lightly damped regressive lead-lag mode of a soft-in-plane hingeless rotor). The loss of stability was predicted using: (a) the same aeroelastic vehicle flight dynamics models that were used in the flight simulator, and (b) transfer functions of the pilot/control device "subsystem" BDFT obtained for the test pilots that performed the flight simulator tests. Several vehicle configurations were flown by two test pilots with somewhat different BDFT transfer functions.

The predictions were substantially confirmed by the tests (Refs. 5, 6). The pilot whose measured BDFT transfer function was predicted to be the most prone to unstable interactions with the vehicle eventually experienced PAO on several occasions, at the expected frequency. The other pilot occasionally experienced only PIO, at a sensibly lower frequency close to the cutoff frequency of human operators.

Presented at the AHS 71st Annual Forum, Virginia Beach, Virginia, May 5–7, 2015.

[1] http://www.aristotel.progressima.eu/

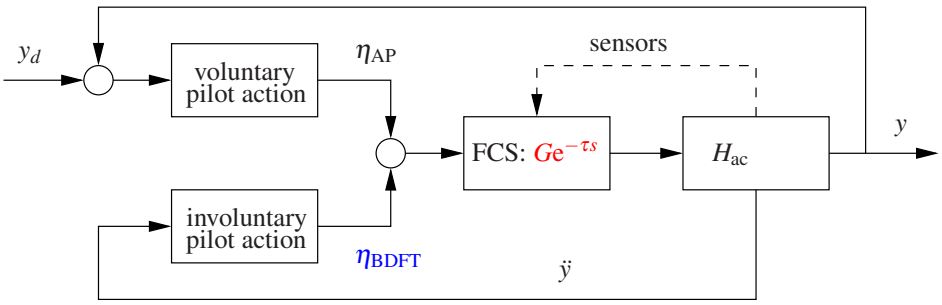

Fig. 1. Block scheme of the feedback loop between the pilot and the helicopter.

DESCRIPTION

The amount and the quality of the data acquired during the previously mentioned campaign made it possible to subsequently identify the transfer functions of the pilots while performing the requested tasks.

Pilot-Vehicle Model Description

The model of the closed-loop system was defined according to the scheme of Fig. 1. Parameters related to both voluntary actions using a crossover-like model (Ref. 7) and involuntary actions were considered. The tested vehicle configurations differed in two ways. The RB model was obtained by statically reducing all of the vehicle states except the six RB states of the AE model. Sensitivity to BDFT was varied by increasing the gain of the lateral cyclic control, G, and by adding a time delay $e^{-\tau s}$ between the inceptor motion η and the control action:

$$\begin{aligned} y &= H_{ac} G e^{-\tau s} \eta = H_{ac} G e^{-\tau s} (\eta_{AP} + \eta_{BDFT}) \\ &= H_{ac} G e^{-\tau s} \left(\overbrace{\frac{1}{G e^{-\tau s} \hat{H}_{ac}} \underbrace{\frac{\omega_c}{s} e^{-\tau_e s}}_{\text{'crossover'}} (y_d - y)}^{\eta_{AP}} + \overbrace{H_{BDFT} s^2 y}^{\eta_{BDFT}} \right) \end{aligned} \tag{1}$$

The voluntary action of the pilot is marginally affected by the varied parameters because pilots are able to adapt to these changes in flight. However, no adaptation was expected to occur with respect to the purely physiological BDFT, since gain and time delay directly multiply the BDFT transfer function in the involuntary control loop. The expected loop transfer function was

$$\begin{aligned} \text{LTF} &= \frac{H_{ac}}{\hat{H}_{ac}} \overbrace{\frac{\omega_c}{s} e^{-\tau_e s}}^{\text{'crossover'}} - s^2 H_{ac} G e^{-\tau s} H_{BDFT} \\ &\cong \underbrace{\frac{\omega_c}{s} e^{-\tau_e s}}_{\text{'crossover'}} - s^2 H_{ac} G e^{-\tau s} H_{BDFT}. \end{aligned} \tag{2}$$

The subsequent analysis indicates that, in some cases, some modification of the BDFT occurred, possibly triggered by the adaptation of the pilot's voluntary action.

Piloted Simulation Flight Tests Description

The pilots were required to perform a variant of the "roll step" maneuver (Fig. 2) developed at the University of Liverpool (Ref. 8). This consists of an initial straight flight path segment along the left-hand side of a runway, followed by a right- and then left-hand turn to fly across the runway towards a series of 'gates' which line up along the right-hand side of the runway. The maneuver is completed by a reciprocal traverse back across the runway whereby the pilot must fly the

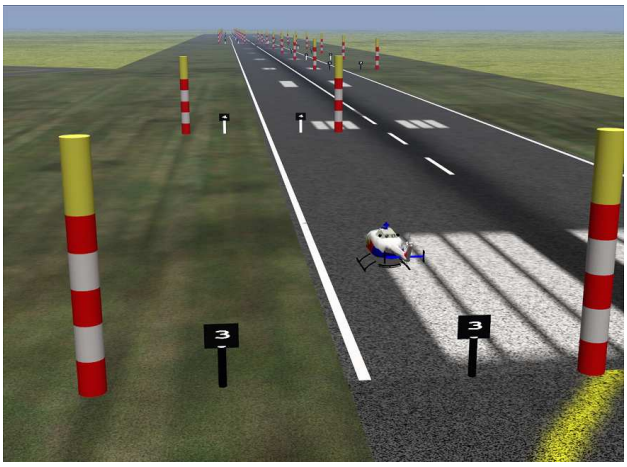

(a) Course layout for Roll Step maneuver.

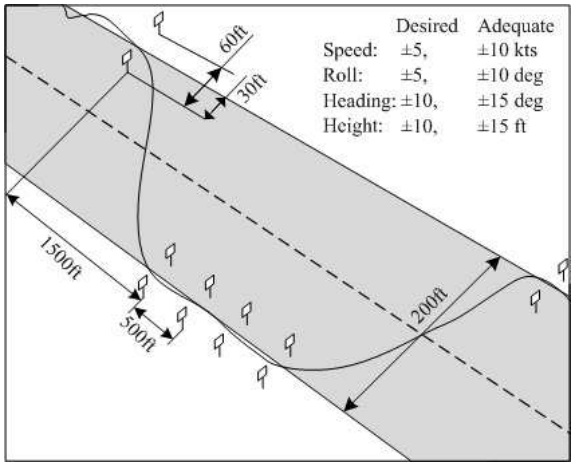

(b) Test course and performance requirements.

Fig. 2. Roll Step MTE description.

Table 1. Tested configurations.

Case	Model	τ, ms	G, n.d.
1	AE	0	1.0
2	AE	0	2.5
3	AE	100	2.5
4	AE	100	3.0
5	RB	100	3.0

vehicle along the left-hand side of the runway once again. It can be decomposed into three phases of straight, level flight, each connected by two turns in opposite directions. Pilots experienced either PAO or PIO during the straight flight phases but no significant adverse oscillations were observed during the turning phases of flight.

Since, during the straight phases of the task, the horizon provided a clear reference for level flight, these can be considered to be precision tracking (i.e. regulatory) tasks. On the contrary, during the turning phases of flight, the pilot is essentially operating in a feedforward mode for most of the duration of the maneuver, returning to a tracking mode only towards the end of each turn.

During the piloted tests, the pilot acted as a component in a feedback loop between the flight simulator and the helicopter model. In this experiment, the last two elements are known, while the transfer function that represents the connection between the pilot cues and the control inputs is the element to be identified.

The analysis focuses on a subset of the piloted simulation flight tests, performed by two test pilots, that were presented in (Refs. 5,6). Five configurations are considered; they are summarized in Table 1. The resulting trajectories, bank angles, and control inceptor deflections are summarized in Figs. 3–5. Each Figure is composed of two subfigures; each subfigure reports data for one of the pilots. Specifically, Fig. 5 reports the motion of the control inceptor scaled by the corresponding gearing ratio scaling factor, G.

In Fig. 3 pilot 1 appears to fly the test course more accurately than pilot 2, as he nearly always achieves the desired trajectory (at least for the test points when the task was successfully completed). Figure 4 shows a similar trend in terms of bank angle. In this case, however, also pilot 1 rarely achieves acceptable performance. Interestingly, when the gain is increased and the time delay is added, pilot 1 appears to start to anticipate the maneuver and initiates it more rapidly and abruptly. This behavior is not observed for pilot 2. It is posited that the observed greater precision for pilot 1 is achieved at the cost of higher gain, which is sufficient to cause a PAO that is not observed with the other, less accurate pilot.

ROVER Analysis

The results have been analyzed using the Real-time Oscillation VERification (ROVER) proposed by Mitchell et al. (Ref. 17). An original implementation of the tool, developed by Mariano et al. in Ref. 18, has been used. The formulation has been adapted to roll by considering the deflection of the lateral cyclic control inceptor, δ_y, and the roll rate, p. Figures 6-10 show the resulting PIO indicators.

Table 2. PIO events detected by ROVER

Case	Pilot 1		Pilot 2	
	PIOR[a]	ROVER	PIOR[a]	ROVER
case 1	2	3	4	3
case 2[b]	4	31	n.a.	15
case 3	n.a.	17	n.a.	31
case 4	4	6[c]	6	35
case 5	1	30	6	46

[a] PIO susceptibility ratings scale (Ref. 21)
[b] this case differs from the actual case 2 in that G_y is 3.0 instead of 2.5, but τ_y is 0.
[c] mission aborted before the second turn

The top portion of each Figure reports the ROVER flags,

1. roll rate p estimated frequency in range $[1,8]$ rad/s;
2. peak-to-peak roll rate p above threshold $p_{\text{thr}} = 18$ deg/s;
3. phase delay between roll rate p and lateral cyclic control inceptor deflection δ_y in range $[-270,-90]$ deg;
4. peak-to-peak lateral cyclic control inceptor deflection δ_y above threshold $\delta_{y_{\text{thr}}} = 7$ %,

and the count of active flags (the circles). When all flags are active, a PIO is detected. The intermediate plot presents the roll rate, p, and the lateral cyclic control inceptor displacement, δ_y. The bottom portion reports the lateral displacement of the helicopter, highlighting the straight phases and the turns.

Table 2 compares the occurrences of PIOs detected by ROVER and the PIO Ratings given by the pilots according to the PIO susceptibility ratings scale reported in Ref. 21. It is worth recalling that such scale is by no means linear; numbers indicate exit points of a conditional path. In synthesis, ratings indicate:

1. no PIO tendency;
2. PIO tendency that can be prevented or eliminated by the pilot;
3. PIO tendency requires considerable pilot attention to be prevented or eliminated, sacrificing task accomplishment;
4. pilot must reduce gain or abandon task to recover from PIO;
5. pilot must open loop to stop PIO after attempting high gain task;
6. PIO tendency when pilot attempts to enter control loop.

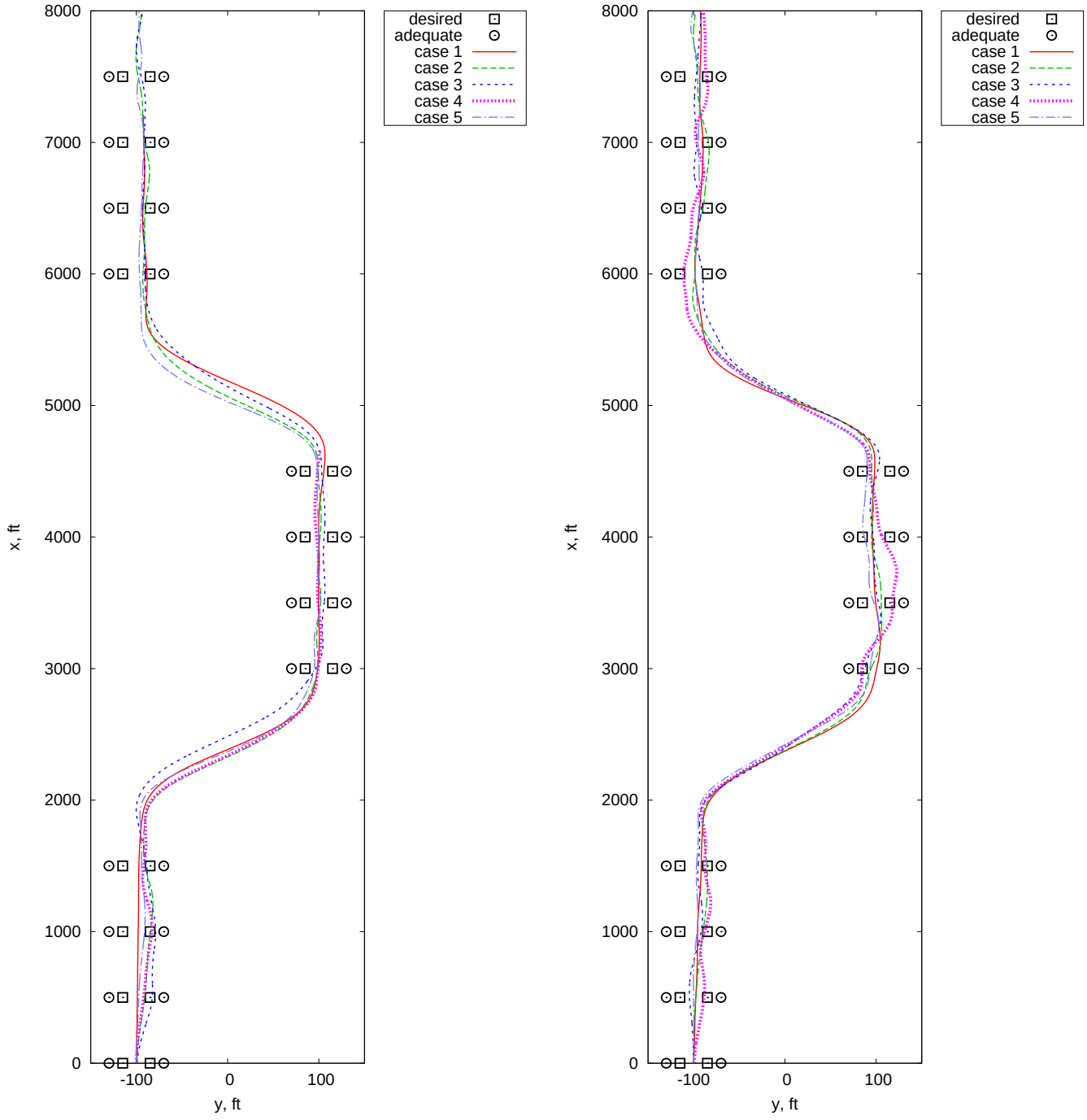

Fig. 3. Trajectories (left: pilot 1; right: pilot 2).

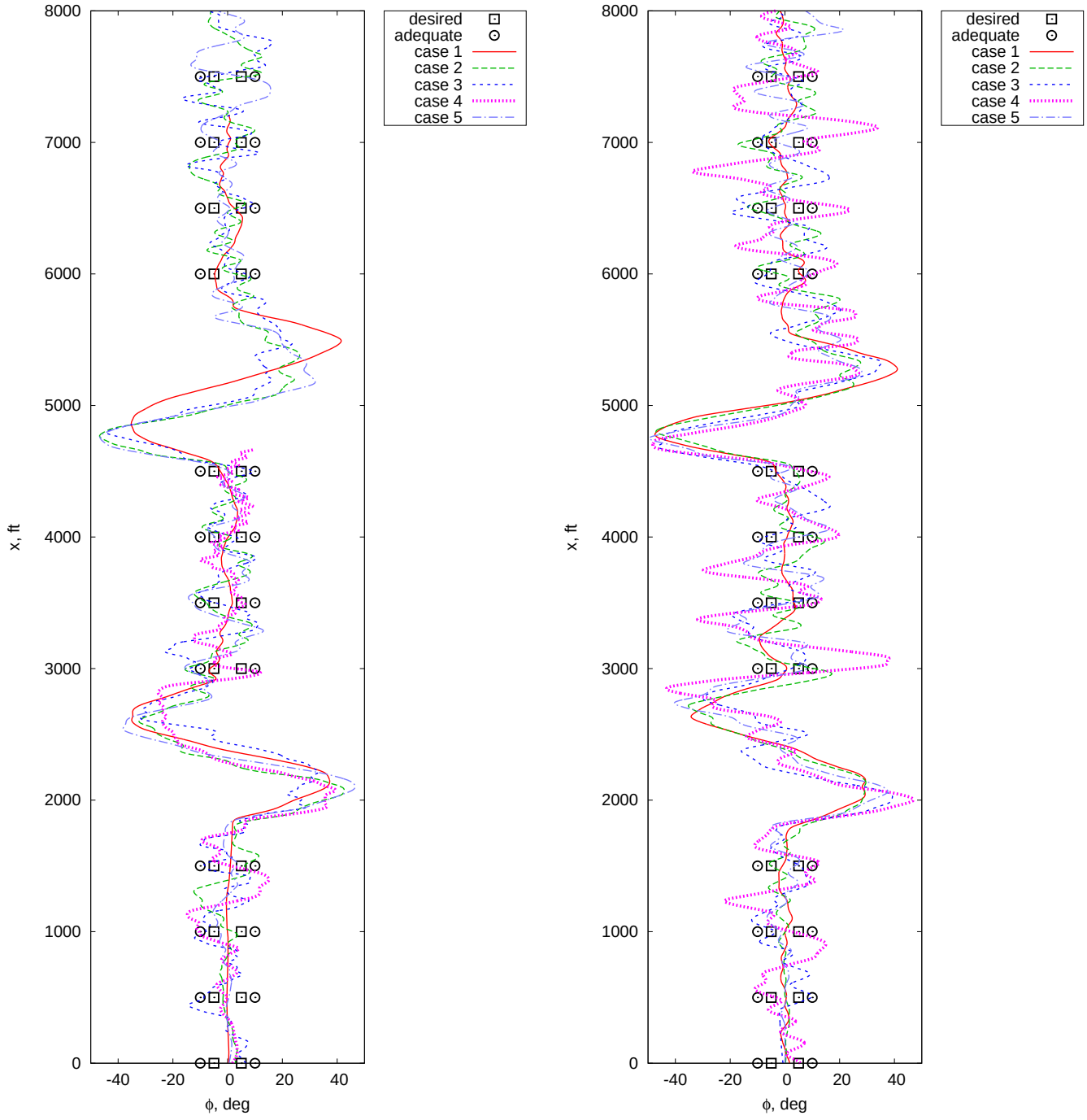

Fig. 4. Bank angles (left: pilot 1; right: pilot 2).

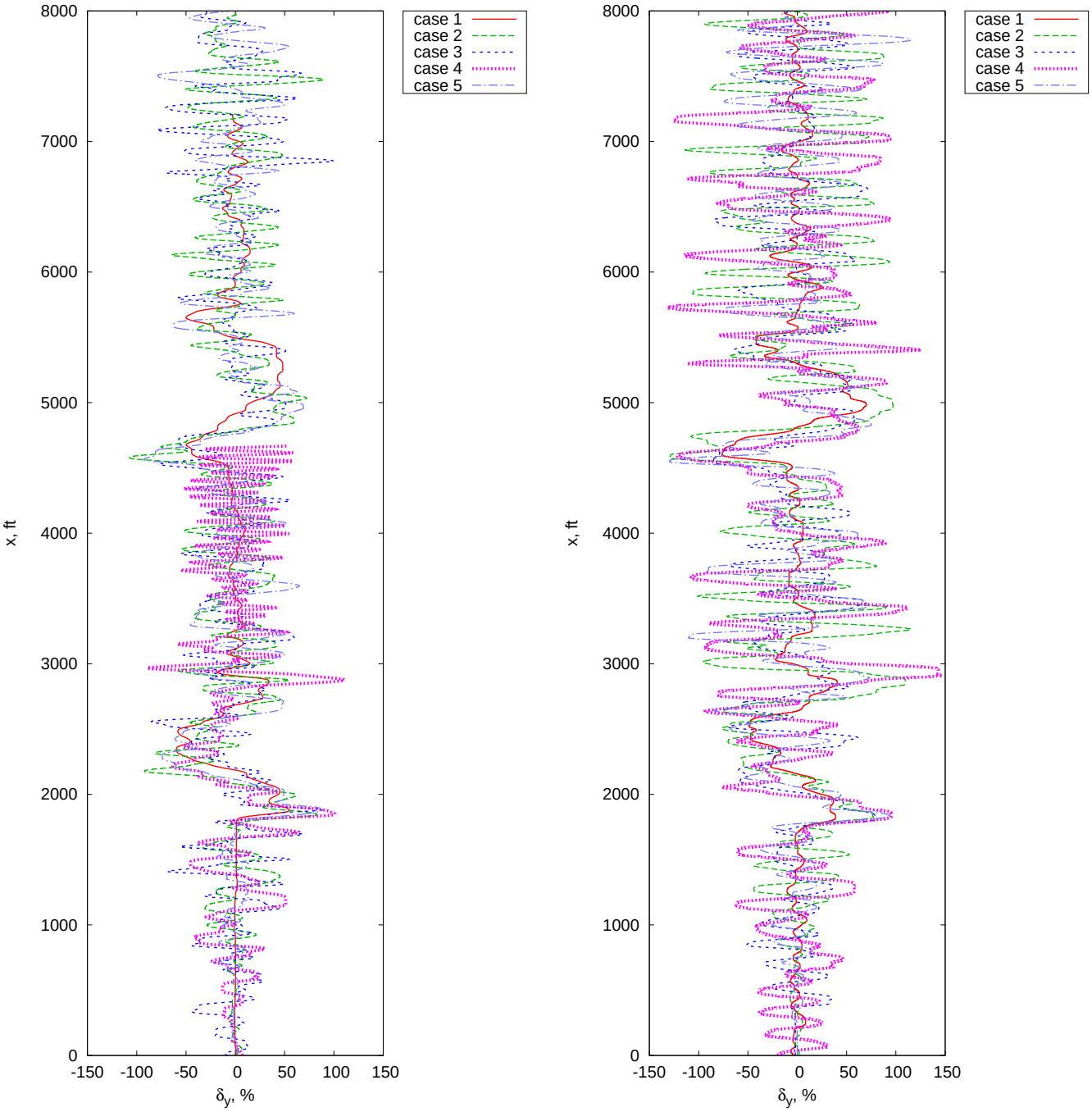

Fig. 5. Lateral cyclic control inceptor deflection times gain (left: pilot 1; right: pilot 2).

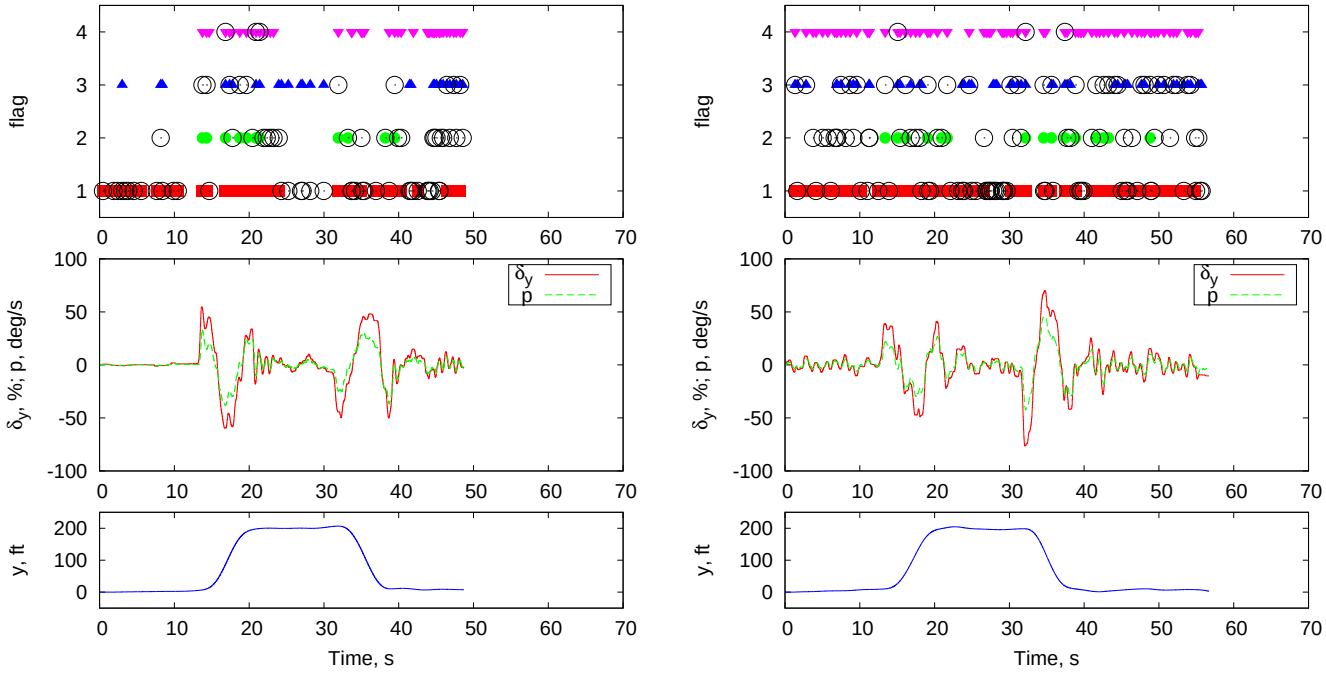

Fig. 6. ROVER applied to case 1, pilots 1 & 2.

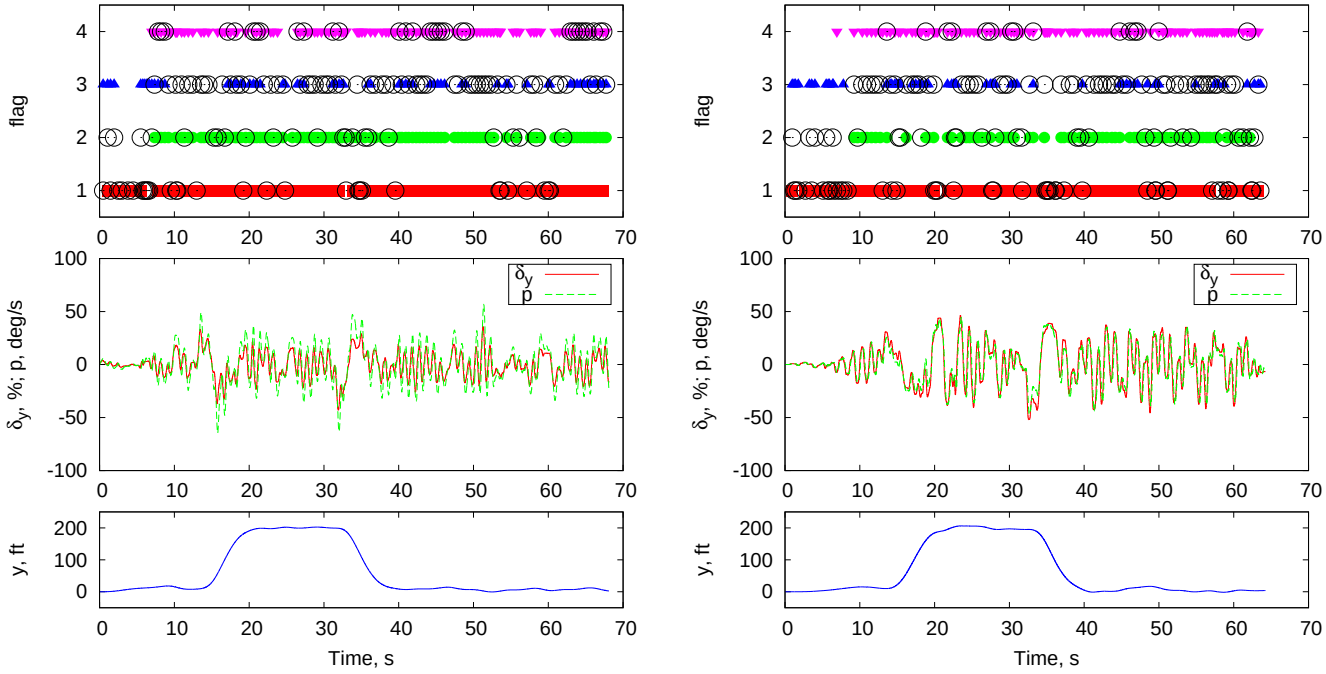

Fig. 7. ROVER applied to case 2, pilots 1 & 2.

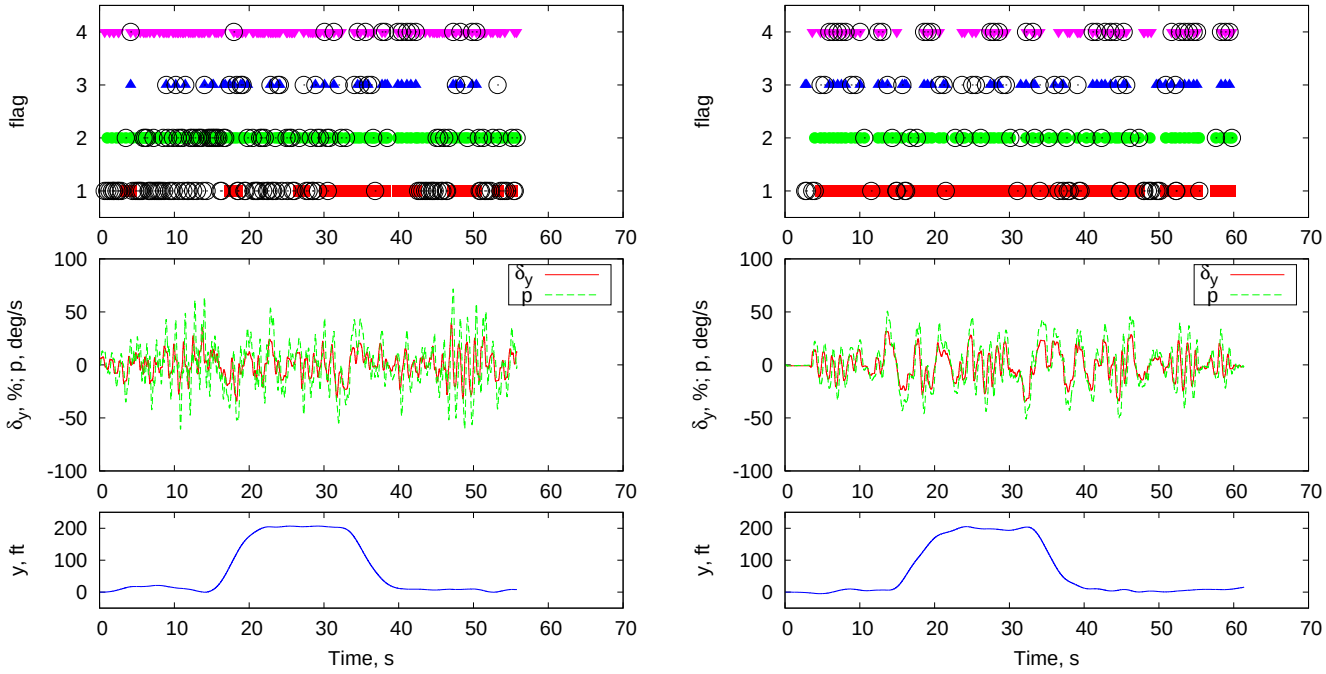

Fig. 8. ROVER applied to case 3, pilots 1 & 2.

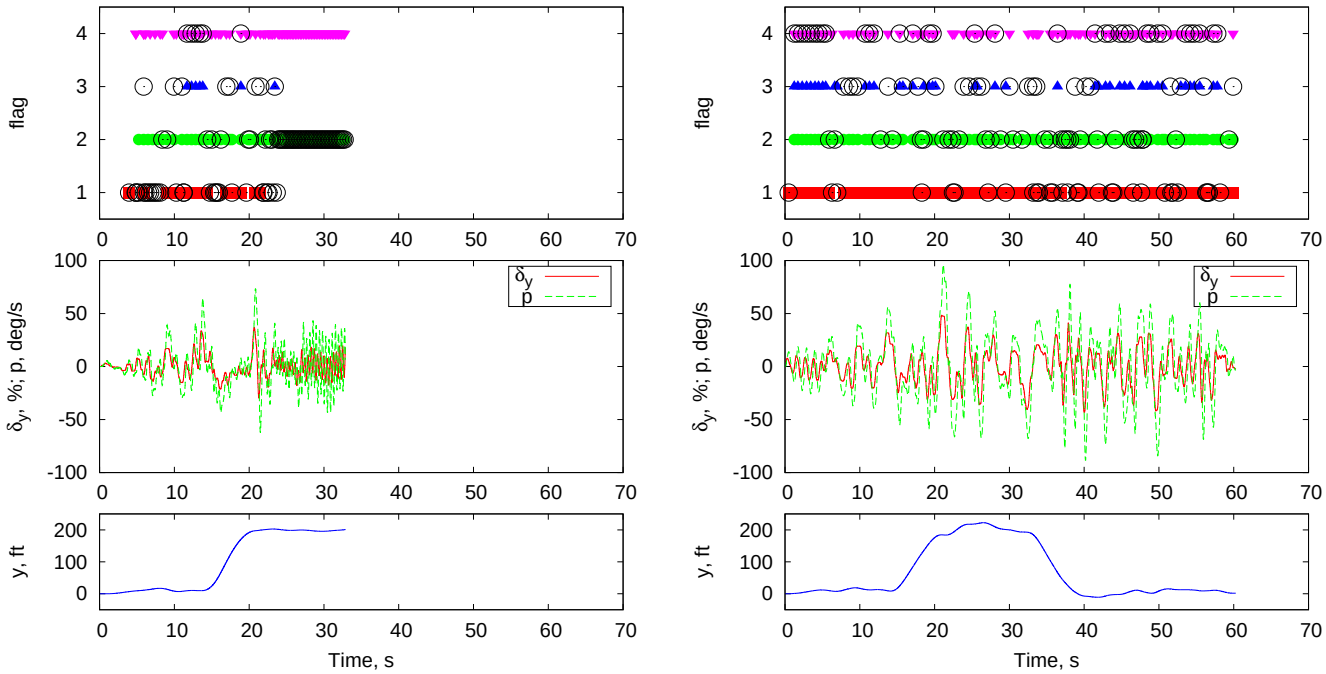

Fig. 9. ROVER applied to case 4, pilots 1 & 2.

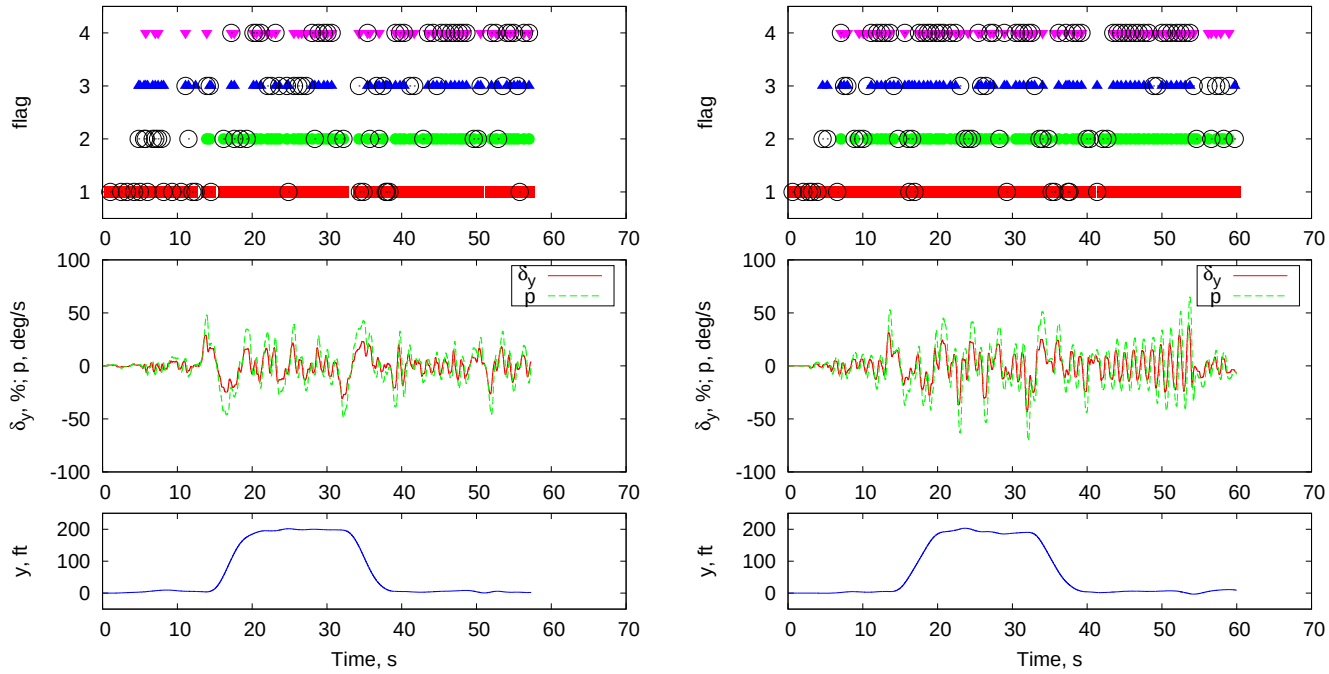

Fig. 10. ROVER applied to case 5, pilots 1 & 2.

There appears to be some correlation between the overall subjective ratings of the pilots and the count of occurrences of PIO according to ROVER.

It is also interesting to note that in case 4, when pilot 1 encounters PAO, ROVER is correctly not predicting a PIO. Indeed, the diverging oscillation that forces the pilot to abandon the task occurs at slightly above 2 Hz, which is outside the band considered in ROVER (1 to 8 rad/s, between about 0.16 and 1.27 Hz).

Pilot 1 rates very poorly the AE vehicle model (PIOR 4) when the gain G_y is higher than nominal (cases 2 and 4), regardless of the presence of the time delay τ_y. The rating is good (PIOR 1) in the nominal configuration of case 1 and, interestingly, in the case of the RB configuration (PIOR 2), despite the very large gain and time delay (case 5). In fact, it was shown in Refs. 5,6 that the PAO experienced by pilot 1 is the result of the adverse interaction of the regressive lead-lag mode of the aircraft's main rotor and the pilot's biodynamics. The RB model does not contain the main rotor lead-lag regressive mode. Apparently, it is such relatively high frequency interaction of aeroelastic nature that causes the poor subjective rating. Pilot 2, instead, is giving a rather consistent poor rating of about 4 and 6 for all configurations. When the time delay in the controls is present, the number of PIOs detected by ROVER is rather high and consistent for pilot 2, whereas ROVER detects less PIOs for pilot 1 in the AE cases with large gain; the least number of PIOs are detected in case 4, which is shorter because the occurrence of a PAO forced the pilot to abandon the task.

PAC Analysis

The Phase-Aggression Criterion (PAC, Ref. 19) has been also used to analyze the results of the piloted simulation tests. The criterion is a measure of active pilot response, incorporating measures of pilot input and vehicle output to infer PIO susceptibility.

In brief, the Aggression A_g is a measure of the pilot's activity in terms of the magnitude of inceptor displacement and rate. The phase Φ is defined as the phase difference between pilot input displacement and vehicle rate output. In principle, the phase is a characteristic of the vehicle that can be inferred from the transfer function between the motion of the control inceptor and the motion of the vehicle.

As the pilot is ultimately interested in achieving a desired attitude, a phase difference of 90 deg between the attitude rate and inceptor input classically describes an out-of-phase response (i.e., the vehicle attitude lags pilot control by 180 deg). Table 3 presents the results in terms of HQ, PIO susceptibility and workload ratings along with the corresponding aggression and phase values for the subset of the planned tests in which AE and RB tested configurations overlapped.

Fig. 11 shows the phase-aggression data related to cases 1–5. Case 1, with nominal gearing ratio and no time delay, shows low values of phase and aggression for both pilots. Case 2, with increased gearing ratio and no time delay, shows a consistent increase of aggression with minimal phase increase. Cases 3 and 4, which differ from case 2 because of added time delay between the control inceptor motion and the actual input, show an increase in aggression and a significant increase of the phase. Case 5, which differs from case 4 for

Table 3. Subjective ratings and objective PIO susceptibility measurements for AE and RB models (excerpt from Ref. 5).

Case	Model	Pilot	τ_y (ms)	G_y (n.d.)	HQ[a] (1–10)	PIOR[b] (1–6)	WL[c] (1–10)	A_G (deg/s)	Phase (deg)
case 1	AE	1	0	1.0	3	2	4	11.0	35.7
case 2[d]	AE	1	0	3.0	5	4	7	72.4	37.4
case 4	AE	1	100	3.0	4	4	8	40.2	55.3
case 5	RB	1	100	3.0	4	1	6	40.2	50.6
case 1	AE	2	0	1.0	5	4	5	23.9	28.1
case 4	AE	2	100	3.0	9	6	9	84.3	55.9
case 5	RB	2	100	3.0	8	6	8	67.5	49.3

[a] Cooper-Harper handling qualities ratings scale (Ref. 20)
[b] PIO susceptibility ratings scale (Ref. 21)
[c] Bedford workload scale (Ref. 22)
[d] this case differs from the actual case 2 in that G_y is 3.0 instead of 2.5, but τ_y is 0.

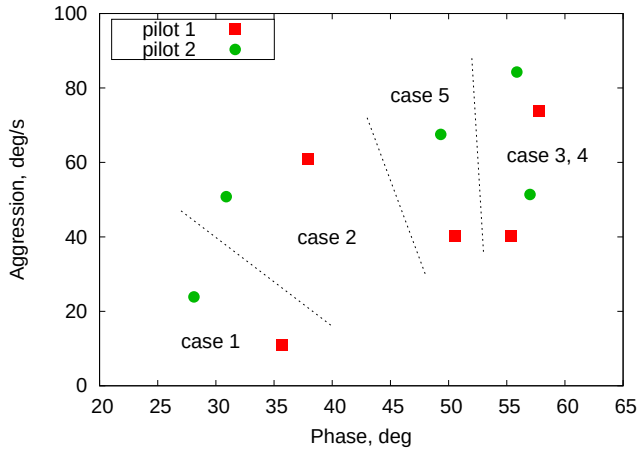

Fig. 11. Phase-aggression levels of cases 1–5.

the elimination of the aeroelastic degrees of freedom, shows a slight reduction of the phase.

Pilot Model Identification

The identification of the voluntary and involuntary pilot models starting from the results collected during closed loop flight simulations is a complex task that requires great care to be accomplished. In fact, special procedures are necessary in order to avoid the main difficulty of closed-loop identification, i.e. the correlation between the disturbances and the control signal, induced by the feedback loop. In this case it was chosen to apply a continuous-time identification algorithm leading directly to models for which each parameter may assume a clear physical meaning (Ref. 9).

In this specific case of the roll step maneuver, a Multiple Input Simple Output (MISO) model was considered for the pilot. The input for the pilot were the yaw angle of the aircraft, the bank angle of aircraft, and the lateral acceleration felt by the aircraft. The latter was specifically intended to represent the input that mainly affects the involuntary control action. The output was the lateral cyclic stick position. The voluntary and the involuntary transfer functions were identified as a single MISO transfer function, with no attempt to separate the involuntary from the voluntary control action.

Several algorithms have been compared for the identification, including the classical N4SID (Ref. 10), the PBSID (Ref. 11), and the RIVCBJ (Refined Instrumental Variable Continuous-time Box Jenkins) (Ref. 9). The latter of these in particular showed itself to be less sensitive to measurement noise and to the noise introduced by the flight simulator motion base actuators. For this reason the RIVCBJ was chosen.

The quality of the identification is not optimal, since the tests were not expressly designed for that specific purpose; nonetheless, clear trends appear, that show an influence of the task and of the vehicle configuration not only on the voluntary behavior, but also on the BDFT (i.e. the involuntary action) of the pilots.

Figure 12 shows the time histories of a PAO event for the pilot that appeared to be prone to PAO, pilot 1, where the shadowed area corresponds to the runway traverse element of the maneuver, while the remainder corresponds to the rectilinear flight paths. This event occurred in the configuration of case 4. Figure 13 shows the results of the identification of pilot 1 in cases 4 and 5, those that show the most significant variations. According to Fig. 13, all contributions to the transfer function that models the pilot change appreciably between adjacent rectilinear phases. The results of the identification show a clear change of the pilot BDFT behavior when comparing the first and second rectilinear phases (see Fig. 13(e)). In particular, in the second phase, the identified transfer function between the roll angle sensed by the pilot and the lateral cyclic input shows a reduction in the frequency at the biodynamic resonant peak. The same analysis conducted with the RB model no longer shows such change in all the three phases considered (Fig. 13(f)).

The plots in Fig. 13(e) clearly show a reduction of the equivalent stiffness of the pilot/control device subsystem in the second rectilinear phase, labeled T2, with respect to the first one, labeled T1. Those plots illustrate the transfer function that expresses the contribution to the control inceptor motion caused by the lateral acceleration of the cockpit, and thus

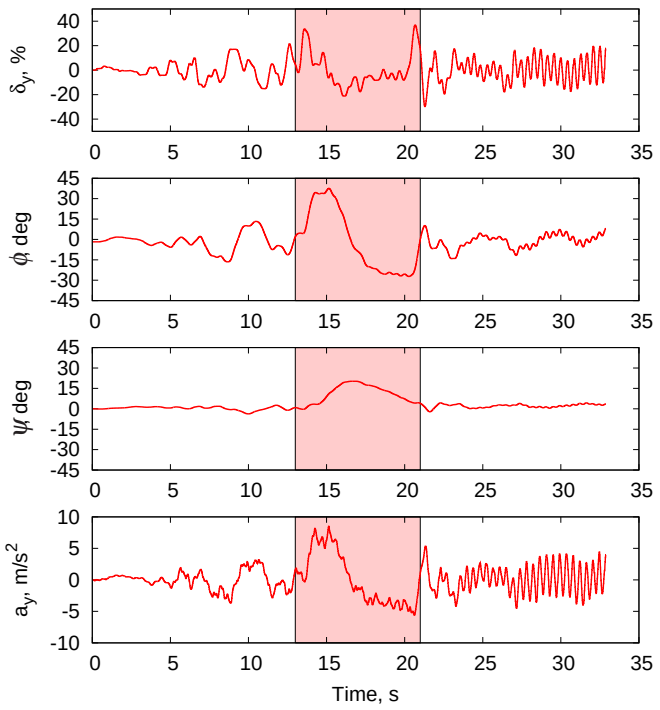

Fig. 12. Time histories of signals during PAO event.

describes the involuntary pilot action (the so-called 'passive pilot').

In fact, in an oversimplified model of the pilot/control device subsystem, which includes the contributions of the control inceptor and of the pilot's biomechanics, the equation of motion of the lateral cyclic control inceptor, whose relative displacement is δ_y, subjected to a lateral acceleration of the cockpit a_y, is

$$\frac{\delta_y}{a_y} = -\frac{m}{s^2 m + sc + k} \tag{3}$$

A reduction of equivalent stiffness k increases the static gain of the transfer function, and shifts the resonance peak towards a lower frequency. This is exactly what is shown in Fig. 13(e).

The identified transfer functions suggest that:

- the BDFT gain appears to *reduce* when the cyclic control input gain G is increased (in contrast with the initial assumption of Eq. (2) that BDFT does not depend on the gain), and thus the phase margin reduces; this suggests that the pilots' reflexive activation changes with the task, and supports the notion that BDFT is task dependent;
- BDFT functions identified during straight and turning phases of flight differ (but turning phases were quite short, with non negligible variations associated with the maneuver, so one can expect identification to be poor in those cases); functions identified during different straight phases of the same flight also differ;
- changes in BDFT based on the task indicate that the pilot transfer function (which can be related to the pilot's reflexive muscular activation, Refs. 12–14) changes when the task requires more precision; this suggests a dependence of the BDFT analogous to that at the root of the Boundary Avoidance Tracking (BAT, Ref. 15) model; i.e., when high *voluntary* gain occurs, muscular activation increases as well;
- the trigger of the PAO observed in case 4 for pilot 1 appears to be a change in BDFT that occurred at the beginning of the second rectilinear phase (at time equal to 21 s in Fig. 12), when the pilot produced a very aggressive lateral control to level the aircraft after the turn. Such acceleration excited the regressive lead-lag motion of the main rotor, which caused pronounced lateral motion at about 2 Hz. The combined transition to a tracking task with high gain, and the need to reduce the aggression on the controls in an attempt to break the control loop causing the PAO produced what has been identified as a reduced equivalent stiffness BDFT, which in turn resulted in a lower biodynamic frequency. This frequency apparently matched the frequency of the lightly damped main rotor regressive lag motion in the non-rotating frame, which resulted in an air resonance-like instability with the pilot in the loop.

In conclusion: the vehicle was prone to PAO thanks to the lightly damped regressive lead-lag motion; pilot 1 had an inherently low biodynamic frequency; the precision tracking task following the turn required high aggression; it is posited that the initiation of the maneuver with high aggression triggered the PAO. System identification shows that after the PAO event was triggered, the BDFT of the pilot (which is related to the involuntary control action) changed in a manner that made the pilot-vehicle system unstable.

DISCUSSION

This work further analyzed the results of a previous piloted flight simulator test campaign that verified predicted PAO instabilities. A novel pilot model is proposed, that combines the low frequency voluntary action with the higher frequency BDFT of the pilot. The models identified from the data obtained in different rectilinear phases of the same roll step maneuver clearly indicate that in critical cases the dynamics of the pilot change in a manner that influences the involuntary action and may eventually result in adverse RPCs.

It is posited that the trigger could be the change in control mode from an essentially open loop operation (the turn to line up with the side of the runway) to a tracking task (flying straight and level through the markers) may trigger the PAO event. The need to precisely track a target could be introduced into the pilot model in a form analogous to the distance from the boundaries (or time to target, Ref. 16) that was proposed by Padfield et al., to trigger changes in the BDFT transfer function.

The currently available data is not sufficient nor adequate to perform a comprehensive and accurate identification of suitable pilot models, mainly because it was not intended for

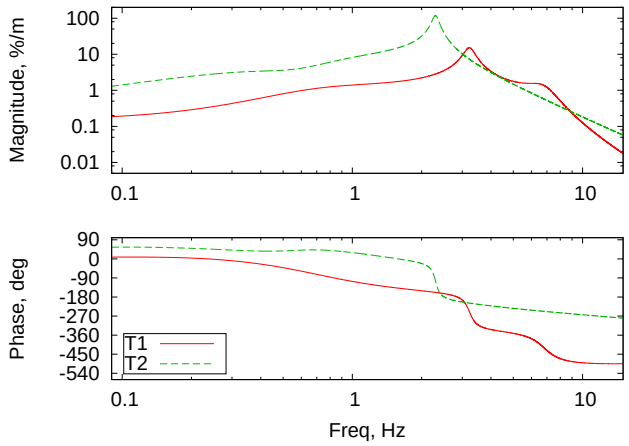

(a) voluntary action, δ_y/lateral position (case 4)

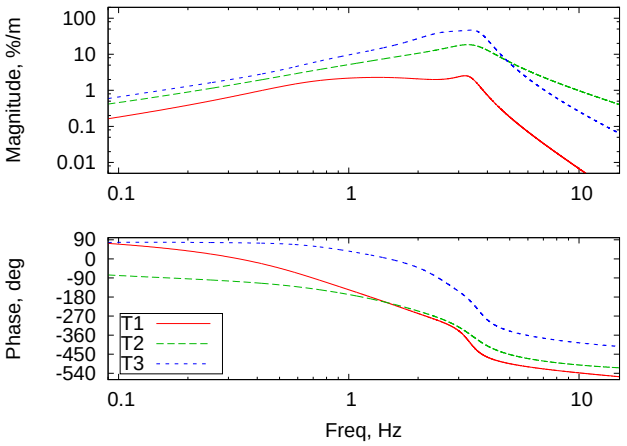

(b) voluntary action, δ_y/lateral position (case 5)

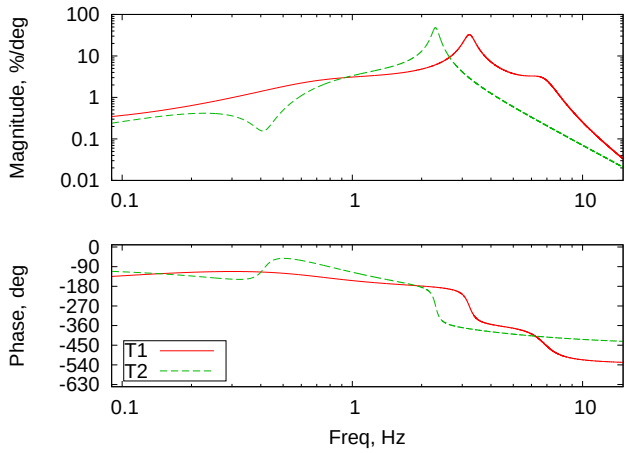

(c) voluntary action, δ_y/bank angle (case 4)

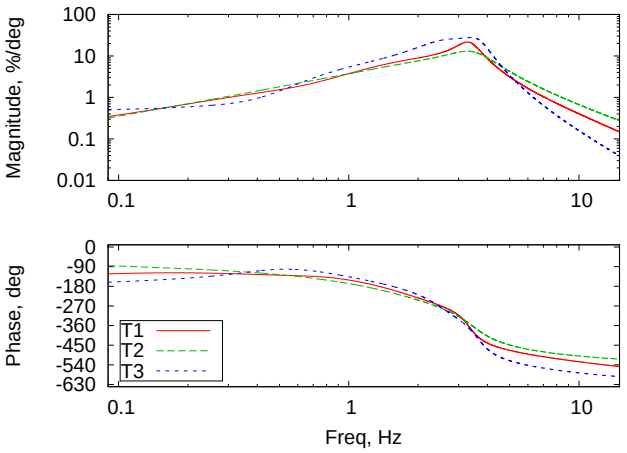

(d) voluntary action, δ_y/bank angle (case 5)

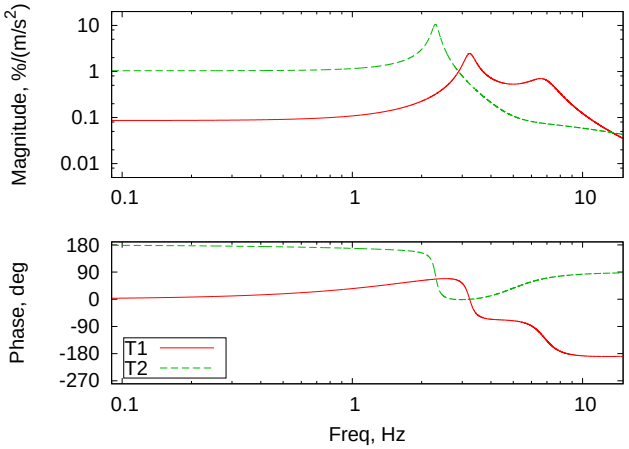

(e) involuntary action, δ_y/lateral acceleration (case 4)

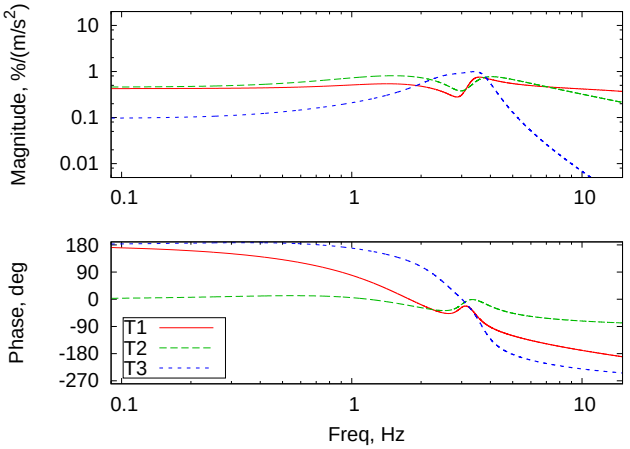

(f) involuntary action, δ_y/lateral acceleration (case 5)

Fig. 13. Identified transfer functions (pilot 1).

such purpose. Nonetheless, it was enough to support the speculations reported in this work, and to suggest that further experiments should be designed and performed in order to collect the required information.

When applied to the results of the piloted simulation flight tests, two methods proposed in the literature for PIO detection (PAC, ROVER) gave results in good agreement with pilot ratings with respect to low-frequency adverse oscillatory events. Regarding PAC, the measure of aggression correctly increased when the gain G was increased; the phase also increased when a time delay was added to the controls. The results obtained with the AE model showed larger phase values than those obtained with the RB one. Regarding ROVER, it gave less positive indications of PIO in the cases that were close to or developed into full PAO for pilot 1; this can be explained by the fact that the oscillations of the PAO event occurred at frequencies outside the band that was monitored by the ROVER algorithm.

The availability of a tool capable of detecting critical oscillatory behaviors of the pilot-vehicle system while discerning between PIO and PAO would be highly desirable. In fact, it could provide more insight into the problem and, if implemented online, it could also be extremely helpful in augmented control vehicles. Such tool should not rely on the careful tuning of thresholds that imply the a priori knowledge of what phenomenon is about to occur; on the contrary, it should be able to provide indications about the frequency content of the phenomena it detects. The definition of the requirements of such a tool is an open problem, let alone its design. Nonetheless, it is believed that the type of piloted simulation flight tests considered in this work would represent a valid motivation and test case for such tool.

CONCLUSIONS

In this work, the results of a piloted simulator flight test campaign originally intended to verify the predicted stability properties of a pilot-vehicle system have been used to identify a model of the pilot. It has been observed that when the instability occurs at a relatively high frequency (about 2 Hz, outside the typical range of pilot-induced oscillations, 1–8 rad/s), the identified transfer function that characterizes the involuntary action of the pilot changes. Specifically, the characteristic biomechanical frequency of the pilot/control device subsystem decreases, and the static response of the biodynamic feedthrough function increases accordingly. These changes are characteristic of a reduction of equivalent stiffness of the pilot/control device subsystem. This change in the biodynamic feedthrough causes the instability of a system that was originally only marginally stable. The trigger of such change is posited to be the change in control mode that occurs at the end of a turn, when the pilot enters a high gain precision tracking task. The identified transfer functions suggest that:

- the biodynamic feedthrough gain appears to reduce when the cyclic control input gain; this suggests that the pilot's reflexive activation changes with the task;
- biodynamic feedthrough functions identified during straight and turning phases of flight differ; functions identified during different straight phases of the same flight also differ;
- changes in biodynamic feedthrough based on the task indicate that the pilot transfer function changes when the task requires more precision.

It must be understood that the tests were not expressly designed to support the identification of the transfer functions of the pilot action; as such, the proposed results may be inaccurate. It is argued that the proposed results suggest the opportunity of further investigation on this subject.

Author contact:
Pierangelo Masarati, pierangelo.masarati@polimi.it;
Vincenzo Muscarello, vincenzo.muscarello@polimi.it;
Giuseppe Quaranta, giuseppe.quaranta@polimi.it;
Paolo Marguerettaz, paolo.marguerettaz@polito.it;
Giorgio Guglieri, giorgio.guglieri@polito.it;
Linghai Lu, linghai.lu@liverpool.ac.uk;
Michael Jump, mjump1@liverpool.ac.uk.

ACKNOWLEDGMENTS

Part of the research leading to these results has received funding from the European Community's Seventh Framework Programme (FP7/2007–2013) under grant agreement N. 323047.

REFERENCES

[1]Pavel, M. D., Jump, M., Dang-Vu, B., Masarati, P., Gennaretti, M., Ionita, A., Zaichik, L., Smaili, H., Quaranta, G., Yilmaz, D., Jones, M., Serafini, J., and Malecki, J., "Adverse rotorcraft pilot couplings — Past, present and future challenges," *Progress in Aerospace Sciences*, Vol. 62, doi:10.1016/j.paerosci.2013.04.003, October 2013, pp. 1–51.

[2]Venrooij, J., Abbink, D. A., Mulder, M., van Paassen, M. M., and Mulder, M., "Biodynamic feedthrough is task dependent," 2010 IEEE International Conference on Systems Man and Cybernetics (SMC), doi:10.1109/ICSMC.2010.5641915, October 10–13 2010.

[3]Pavel, M. D., Malecki, J., DangVu, B., Masarati, P., Gennaretti, M., Jump, M., Jones, M., Smaili, H., Ionita, A., and Zaicek, L., "Present and Future Trends in Aircraft and Rotorcraft Pilot Couplings — a Retrospective Survey of Recent Research Activities within the European Project ARISTOTEL," 37th European Rotorcraft Forum, Paper no. 116, September 13–15 2011.

[4]Pavel, M. D., Malecki, J., DangVu, B., Masarati, P., Gennaretti, M., Jump, M., Smaili, H., Ionita, A., and Zaicek, L., "A Retrospective Survey of Adverse Rotorcraft Pilot Couplings in European Perspective," American Helicopter Society 68th Annual Forum, May 1–3 2012.

[5]Muscarello, V., Masarati, P., Quaranta, G., Lu, L., Jump, M., and Jones, M., "Investigation of Adverse Aeroelastic Rotorcraft-Pilot Coupling Using Real-Time Simulation," American Helicopter Society 69th Annual Forum, Paper No. 193, May 21–23 2013.

[6]Muscarello, V., Quaranta, G., Masarati, P., Lu, L., Jones, M., and Jump, M., "Prediction and Simulator Verification of Roll/Lateral Adverse Aeroservoelastic RotorcraftPilot Couplings," *J. of Guidance, Control, and Dynamics*, doi:10.2514/1.G001121, in press.

[7]McRuer, D. T. and Jex, H. R., "A Review of Quasi-Linear Pilot Models," *Human Factors in Electronics, IEEE Transactions on*, Vol. HFE-8, (3), doi:10.1109/THFE.1967.234304, September 1967, pp. 231–249.

[8]Cameron, N. and Padfield, G. D., "Handling Qualities Degradation in Tilt-Rotor Aircraft Following Flight Control System Failures," 30th European Rotorcraft Forum, September 14-16 2004.

[9]Jones, M., Jump, M., Lu, L., Yilmaz, D., and Pavel, M. D., "Using the Phase-Aggression Criterion to Identify Rotorcraft Pilot Coupling Events," 38th European Rotorcraft Forum, September 3–7 2012.

[10]Mitchell, D., Arencibia, A., and Munoz, S., "Real-Time Detection of Pilot-Induced Oscillations," AIAA Atmospheric Flight Mechanics Conference and Exhibit, AIAA-2004-4700, August 16–19 2004.

[11]Mariano, V., Guglieri, G., and Ragazzi, A., "Application of pilot induced oscillations prediction criteria to rotorcraft," American Helicopter Society 67th Annual Forum, May 3–5 2011.

[12]Jones, M., Jump, M., and Lu, L., "Development of the Phase-Aggression Criterion for Rotorcraft Pilot Couplings," *J. of Guidance, Control, and Dynamics*, Vol. 36, (1), doi:10.2514/1.58232, January-February 2013, pp. 35–47.

[13]Cooper, G. E. and Harper, R. P., "The Use of Pilot Rating in the Evaluation of Aircraft Handling Qualities," TN D-5153, NASA, April 1969.

[14]Roscoe, A. and Ellis, G., "A subjective rating scale for assessing pilot workload in flight: A decade of practical use," TR 90019, Royal Aerospace Establishment, 1990.

[15]Garnier, H. and Wang, L., *Identification of Continuous-time Models from Sampled Data*, Springer, 2008.

[16]Overschee, P. V. and Moor, B. D., "N4SID: Subspace algorithms for the identification of combined deterministic-stochastic systems," *Automatica*, Vol. 30, (1), doi:10.1016/0005-1098(94)90230-5, 1994, pp. 75–93.

[17]Bergamasco, M. and Lovera, M., "Continuous-time predictor-based subspace identification using Laguerre filters," *IET Control Theory & Applications*, Vol. 5, (7), doi:10.1049/iet-cta.2010.0228, 2011, pp. 856–867.

[18]Masarati, P., Quaranta, G., Bernardini, A., and Guglieri, G., "A voluntary/involuntary pilot model for helicopter flight dynamics and aeroservoelasticity," AIAA Modeling and Simulation Technologies Conference, June 16–20 2014.

[19]Masarati, P., Bindolino, G., and Quaranta, G., "A Parametric Pilot/Control Device Model for Rotorcraft Biodynamic Feedthrough Analysis," 40th European Rotorcraft Forum, September 2–5 2014.

[20]Masarati, P., Quaranta, G., Bernardini, A., and Guglieri, G., "A Multibody Model for Piloted Helicopter Flight Dynamics and Aeroservoelasticity," *J. of Guidance, Control, and Dynamics*, Vol. 38, (3), doi:10.2514/1.G000837, 2015, pp. 431–441.

[21]Gray, W. R., III, "Boundary Avoidance Tracking: A New Pilot Tracking Model," AIAA Atmospheric Flight Mechanics Conference and Exhibit, AIAA 2005-5810 doi:10.2514/6.2005-5810, August 15–18 2005.

[22]Padfield, G. D., Lu, L., and Jump, M., "Tau Guidance in Boundary-Avoidance Tracking - New Perspectives on Pilot-Induced Oscillations," *J. of Guidance, Control, and Dynamics*, Vol. 35, (1), doi:10.2514/1.54065, 2012, pp. 80–92.